ASTRONOMY & ASTROPHYSICS
SUPPLEMENT SERIES

Astron. Astrophys. Suppl. Ser. **62**, 279-290 (1985)

Spectrophotometry of peculiar B and A stars. XVIII. The helium rich variable stars HR 1890, Sigma Orionis E, and HD 37776

S. J. Adelman ([1,2,*]) and D. M. Pyper ([3,*])

([1]) Department of Physics, The Citadel, Charleston, SC 29409, U.S.A.
([2]) Laboratory for Astronomy and Solar Physics (**), Code 681, NASA Goddard Space Flight Center, Greenbelt, MD20771, U.S.A.
([3]) Department of Physics, University of Nevada, Las Vegas, NV 89154, U.S.A.

Received April 15, accepted May 7, 1985

Summary. — Optical region spectrophotometry of $\lambda\lambda$3300-7850 has been obtained for three helium rich stars, HR 1890, σ Ori E, and HD37776, of the Orion OB1 Association. New *uvbyβ* photometry of HR 1890 and HD 37776 as well as published data are also used to investigate the variability of these stars. A new period of 1.53862 days was determined for HD 37776. For all three stars Hβ varies in antiphase with strong He I lines. The spectrophotometric bandpass containing the strong He I line λ4471 varies in phase with the *R* index of Pedersen and Thomsen. Evidence is found for weak absorption features which appear to be an extension of the λ5200 feature seen in cooler CP stars.

Key words : helium variable stars — spectrophotometry.

1. Introduction.

The helium rich variable stars are a class of main sequence peculiar B stars which have enhanced helium abundances, spectrum variability, and strong magnetic fields (Borra and Landstreet 1979; Pedersen, 1979). They appear to be an extension of the magnetic peculiar A stars, to temperatures between approximately 18000 K and 25000 K (Osmer and Peterson, 1974; Hunger, 1976; Shore, 1978; Lester, 1979). In this paper we study three members of the Orion OB1 Association which have rotational periods of less than 1.6 days and apparent rotational velocities near 150 km s^{-1}: HR 1890 (= HD 37017), σ Orionis E (= HD 37479 = HR 1932), and HD 37776. Their helium line variability is periodic (Pedersen and Thomsen, 1977; Pedersen, 1979) with the magnetic and spectroscopic periods in agreement (Landstreet and Borra, 1978; Borra and Landstreet, 1979). These stars also display Hα emission and light variability in the same period (Walborn and Hesser, 1976; Pedersen, 1979). Walborn (1983) discusses the morphology of this class of stars.

IUE observations of HR 1890, σ Ori E, and HD 37776 show that the He I variations are in anti-phase with those of carbon, silicon, and aluminum and that these lines vary periodically with the rotational timescale. Weak stellar winds are present which also vary in the same period (Shore and Adelman, 1981). The Si II, Si III, and Si IV lines in combination with Kamp's (1978) analysis indicate temperatures of 18000 K, 24100 K, and 20600 K for HR 1890, σ Ori E, and HD 37776, respectively.

2. Observations and results.

Scans of HR 1890, σ Ori E, and HD 37776 were obtained with the HCO Scanner on the #1 92-cm telescope at Kitt Peak National Observatory (KPNO) primarily in the fall of 1980 and the winter of 1981. The data reduction procedures are those of Adelman (1978) with the calculation of the synthesized *u-b* and *b-y* colors as modified by Adelman and Pyper (1983) and that of the broad, continuum feature indices and the *hb* index as given by Pyper and Adelman (1983).

For the He-rich stars, the λ4200 absorption feature indices are not useful, as the magnitudes of $\lambda\lambda$4032 and 4464 are affected by the strong He I lines at λ4026 and λ4472. To examine possible absorption near λ4200, we introduce a new index

$$ih^* = m_{4167} + m_{4200} - 1.497\, m_{4055} - 0.503\, m_{4566}\,.$$

Inspection of the energy distributions showed the bandpasses centered at λ4055 and λ4566 to be continuum points relatively unaffected by absorption. Also, the index $\Delta a'$ is of limited usefulness, as examination of the individual scans shows little or no absorption at λ5264 and absorption only in the $\lambda\lambda$4935-5128 region. Thus an analogous index

(*) Visiting Astronomer, Kitt Peak National Observatory, National Optical Astronomy Observatories, operated by the Association of Universities in Research in Astronomy, Inc., under contract with the National Science Foundation.
(**) NRC-NASA Research Associate.

Send offprint requests to : Dr. Adelman at Goddard address.

$$ah' = m_{5000} + m_{5060} + m_{5128} - 2.547\, m_{4975} - 0.4526\, m_{5556}$$

is also introduced, using the wavelengths at which the greatest absorption occurs and the continuum points that seem most free of absorption in all scans. These indices cannot be properly compared with those of normal stars due to insufficient observations of the latter, but they are useful for variation studies. We have scans of two normal stars at almost the same wavelength density as those of the three He stars : HR 1861 (B1V) in the blue and η UMa (B3V) in the red. The appropriate index values for these stars are $ih^* = 0.036$ mag for HR 1861 and $ah' = 0.043$ mag for η UMa.

Table I is the journal of observations for all three program stars. The phases are based on the ephemerides given below. Tables II, III, and IV contain the individual and average energy distributions as well as the values of the various indices for HR 1890, σ Ori E, and HD 37776, respectively. These three stars, as members of the Orion OB1 Association, are slightly reddened. Warren and Hesser (1978) found that the $E(b\text{-}y)$ values are 0.06 mag, 0.06 mag, and 0.08 mag for HR 1890, σ Ori E, and HD 37776, respectively. Along with the spectrophotometric scans we have included a dereddened average energy distribution for each star. The interstellar reddening law of Schild (1977) was used. These tables also contain the synthesized colors and feature indices, including the Hβ indices *hb* (Pyper and Adelman, 1983) for the three stars. The second order bandpasses are 20 Å for the winter 1981 observations and 30 Å for the remaining observations.

The *uvbyβ* photometry of HR 1890 and HD 37776 by DMP was obtained from 1981 to 1984 using the #4 41 cm telescope at KPNO. Reductions were done at UNLV following the procedures of Crawford and Barnes (1970) and Crawford and Mander (1966), using modified KPNO software. Table V contains a summary of the four-color observations of the three stars compared with the synthesized spectrophotometric *u-b* and *b-y* values. Also included in this table are the average photometric values of DMP for HR 1890, HD 37776, and their comparison stars. Table VI contains the individual four-color values of DMP for HR 1890 and HD 37776.

Both the mean *u-b* values for the spectrophotometry and the mean photometric values of DMP average bluer (larger Balmer jump) than those values previously published. These systematics probably reflect differences in ultraviolet extinction and photometric filters at different observatories. These helium stars are about as hot as any of the normal stars used in the calibration of the synthesized *u-b* and *b-y* colors (see Adelman and Pyper, 1983) and only a few such stars were observed. This makes the calibration somewhat uncertain in this temperature range. In most cases the values compare within 2 σ of the DMP averages. The synthetic *b-y* averages do not differ significantly from the photometric values for any of the three helium stars. The observations of the individual stars are discussed in more detail below.

HR 1890 : The average energy distribution is quite smooth for HR 1890 (Fig. 1). Certain magnitudes such as those centered at λ4032 and λ4464 are fainter than adjacent values due to the presence of strong He I lines in the bandpass. There is a slight depression in the continuum values between $\lambda\lambda$5000-5200 relative to the trend of Paschen continuum values. The λ3448 value is always fainter than adjacent values in the Balmer continuum. Except for the possible change in the size of the Balmer jump, examination of the spectrophotometry does not reveal much evidence for variability other than some changes in those bandpasses affected by strong He I lines.

The four-color photometry of DMP (Fig. 2) confirms the period of HR 1890 determined by Pedersen (1979) from the He I spectrum variations. The ephemeris is :

$$\text{JD (He I maximum)} = 2442812.23 + 0.90117\, E\,.$$

For HR 1890, the synthesized *b-y* values as a function of phase (Fig. 3) show little evidence of variation and reinforce the photometric data of Pedersen and Thomsen (1977) and DMP (this paper) which show that this color is nearly constant. Also the spectrophotometric *u-b* values reinforce the photometry which indicates low amplitude variability (Fig. 3). The *u-b* value for scan 2 is below the trend of synthesized colors as its values shortward of λ3571 are fainter than those of adjacent scans in phase. The Δa index indicates the absence of this features and shows no clear evidence of variation with phase. The ih^* and ah' indices may vary in phase with the He I lines but the scatter is large. The β and *hb* indices indicate that Hβ varies in antiphase with the He I lines.

Sigma Orionis E : Sigma Ori E exhibits a wide range of interesting phenomena. Of particular note is a double minimum light curve (Hesser *et al.*, 1977) combined with an apparently constant radial velocity (Bolton, 1974) and complex He I variations (Pedersen, 1979).

As σ Ori E is very close to the four other early type stars in the σ Ori system, one has to be very careful in correcting for the sky background when making spectrophotometric observations. If too large an aperture is used or the comparison channel is placed in a location not equally contaminated by scattered light from the other stars in the system, then the observations can be in error. These difficulties are more serious for the Balmer continuum than for the Paschen continuum. To check for such problems we compared the synthesized *u-b* and *b-y* colors with those of Hesser *et al.* (1977). Almost all of the *b-y* values were in reasonable agreement, but a number of scans had discrepant *u-b* values, and were excluded. We are reasonably certain that the 14 remaining scans are of good photometric quality.

In figure 4, we show the synthesized colors and absorption feature indices as a function of phase. Following Hesser *et al.* (1977), who obtained *uvbyβ* photometry of σ Ori E, we use the ephemeris

$$\text{JD (primary light minimum)} = 2442778.819 + 1.19081\, E\,.$$

Unfortunately we do not have scans at exactly primary and secondary minima (phases 0.0 and 0.4, respectively) although we have some which are close to these minima. Except for *b-y* and *u-b*, the indices are plotted with the large values (greatest strength of the feature) at the top. The *b-y* values of Hesser *et al.* (1977) are almost constant as a function of phase, with a scatter of 0.005 mag (1 σ rms) about the mean. The spectrophotometric *u-b* values also agree with those of Hesser *et al.* including the eclipse phases. The Δa index of the average scan indicates that the λ5200 broad absorption feature seen in the magnetic Ap stars is absent. However, 10 of the 12 scans have *ah'* values greater than that of η UMa whereas only 8 of the 12 scans have *ih** values greater than that of HR 1861. The latter two indices show a large scatter when plotted *vs.* phase and none of the three indices show evidence of variations with phase. The *hb* index appears to agree with the β measurements of Hesser *et al.* in that these values show a minimum near phase 0.9, which is the phase of the He I maximum.

Figure 1 shows the average energy distribution of σ Ori E as observed and as corrected for reddening. The shapes of both energy distributions are rather similar. Certain magnitudes which are fainter than the trend of adjacent values are definitely affected by strong He I lines, in particular m_{4032} by λ4026 and m_{4464} by λ4472. On individual scans these values are found to be variable. For $\lambda\lambda$5000-5200 the continuum appears to be slightly depressed relative to the trend of adjacent values. The shape of the Balmer continuum is unusual compared with normal and Ap stars. The λ3571 value is brighter than the trend of adjacent values and there is a change in slope near λ3448. There are some apparent changes in shape from scan to scan, but this region is more affected than is the Paschen continuum by both scattered light and extinction corrections.

HD 37776 : For HD 37776, as for HR 1890, the average energy distribution is quite smooth with the magnitudes affected by strong He I lines below the trend of those continuum values which are not so affected. Again the λ3448 value is almost always fainter than adjacent values in the Balmer continuum, while on most scans the λ3571 value is brighter than adjacent values. There are suggestions of a slight depression of the λ5200 region for most scans.

A comparison of the recent *uvbyβ* photometry of DMP with that of Pedersen and Thomsen (1977) shows that an adjustment must be made in the 1.5385 day period of HD 37776 determined by Pedersen (1979). The best fit to the photometric data (Fig. 5) is for a slightly longer period given by the ephemeris

$$\text{JD (He I minimum)} = 2442808.59 + 1.53862\,E.$$

The adjusted *u-b* and *b-y* spectrophotometric values correspond fairly well to the photometric values and reinforce the suggestion of slight variability (Fig. 6). The Δa index indicates the absence of the λ5200 absorption feature. The *ah'* index has 13 of 17 values greater than that of η UMa and appears to show a variation in antiphase with that of the He I lines, although the scatter is large. The average *ih** index value is about the same as that for HR 1861 and the individual values show no clear evidence of variability with phase. Both the β values and the *hb* values show a variation of Hβ in antiphase with the He I lines.

3. Discussion.

The use of Kurucz's (1979) fully line blanketed solar composition models to estimate temperatures can lead only to an approximate calibration as the stellar abundances, particularly helium, are non-solar. If we assume $\log g = 4.0$, then we find for HR 1890, σ Ori E, and HD 37776 ; 20000 K, 23400 K, and 22500 K, respectively (Fig. 1). However, this value of $\log g$ may be too small and $\log g = 4.5$ may be more appropriate, which is the case for main sequence early B stars. For example, for σ Ori E, even though the He/H ratio is non-solar and variable, the predictions of a 24200 K, $\log g = 4.5$ model fit the entire optical region except for a few points. Without a gravity indicator it is almost impossible to choose the temperature uniquely.

The shapes of the Balmer continua of these stars are somewhat different from those of the models which have solar helium abundances. All three stars show m_{3448} to be fainter than the continuum and in σ Ori E there is a change in slope of the continuum near this wavelength. This is apparently due to the λ3422 He I bound-free discontinuity. Further the comparison of stellar values and model predictions show the presence of very weak continuum absorption between λ4975 and λ5200. This limited wavelength interval is displaced from the location of the λ5200 feature in the classical types of magnetic Ap stars. To check whether it is due to He absorption lines, we examined the magnitudes at wavelengths near the three strong He I lines in the region $\lambda\lambda$4400-5200, which are at λ4472, λ4935, and λ5015. These He I lines are all presumably variable in phase with λ4026, measured photoelectrically as an index *R* by Pedersen and Thomsen (1977) and Pedersen (1979). We calculated three indices measuring an absorption below a « continuum » line interpolating the brightest nearby points, which are defined as :

$$h_1 = m_{4464} - 0.5\,(m_{4412} + m_{4566}),$$
$$h_2 = m_{4935} - 0.5\,(m_{4785} + m_{4975}),$$
$$h_3 = m_{5000} - 0.957\,m_{4975} - 0.043\,m_{5556},$$

and measured the effects of λ4472, λ4922, and λ5015, respectively. As seen in figure 7, the h_1 variations closely follow those of *R* measured by Pedersen and Thomsen, while the h_2 and h_3 indices show weak or no variations in phase with *R*. Since the m_{5060} and m_{5128} values are also usually depressed as well as the m_{5000} value, and there are no strong He I lines near these former two wavelengths, the absorption feature in this wavelength region cannot be entirely due to He I absorption. Thus it might be due to a high temperature analog or extension of the λ5200 feature seen in cooler magnetic Ap stars. For σ Ori E, the best studied of these three stars, our observations support the predictions of a unified model, based on the oblique rotator model (ORM) and radiative diffusion, for the helium peculiar stars according to which σ Ori E has a helium rich band surrounding the magnetic equator (Shore, 1978 ; Shore and Bolton, 1985).

Acknowledgements.

We would like to thank the Director of Kitt Peak National Observatory, National Optical Astronomy Observatories, for the observing time needed to do this study. This research was supported in part by The Citadel Development Foundation and the Department of Physics, University of Nevada, Las Vegas.

References

ADELMAN, S. J. : 1978, *Astrophys. J.* **222,** 547.
ADELMAN, S. J., PYPER, D. M. : 1983, *Astrophys. J.* **266,** 732.
BOLTON, C. T. : 1974, *Astrophys. J. Lett.* **192,** L7.
BORRA, E. F., LANDSTREET, J. D. : 1979, *Astrophys. J.* **228,** 809.
CRAWFORD, D. L., BARNES, J. V. : 1970, *Astron. J.* **75,** 978.
CRAWFORD, D. L., BARNES, J. V., GOLSON, J. C. : 1971, *Astron. J.* **76,** 1058.
CRAWFORD, D. L., MANDER, J. : 1966, *Astron. J.* **71,** 114.
GRØNBECH, B., OLSEN, E. H. : 1976, *Astron. Astrophys. Suppl. Ser.* **25,** 213.
HESSER, J., MORENO, H., UGARTE, P. : 1977, *Astrophys. J. Lett.* **216,** L31.
HUNGER, K. : 1976, in *Stellar Atmospheres and Envelopes,* eds B. Baschek, W. Kegel, G. Traving (Springer-Verlag, NY) p. 57.
KAMP, L. W. : 1978, *Astrophys. J. Suppl.* **36,** 143.
KILKENNEY, D. : 1978, *Monthly Notices Roy. Astron. Soc.* **182,** 629.
KURUCZ, R. L. : 1979, *Astrophys. J. Suppl.* **40,** 1.
LANDSTREET, J. D., BORRA, E. F. : 1978, *Astrophys. J. Lett.* **224,** L5.
LESTER, J. D. : 1979, *Astrophys. J.* **233,** 644.
OSMER, P. S., PETERSON, D. M. : 1974, *Astrophys. J.* **187,** 117.
PEDERSEN, H. : 1979, *Astron. Astrophys. Suppl. Ser.* **35,** 313.
PEDERSEN, H., THOMSEN, B. : 1977, *Astron. Astrophys. Suppl. Ser.* **30,** 11.
PYPER, D. M., ADELMAN, S. J. : 1983, *Astron. Astrophys. Suppl. Ser.* **51,** 365.
SCHILD, R. E. : 1977, *Astron. J.* **82,** 337.
SHAW, J. S. : 1975, *Astron. Astrophys.* **41,** 367.
SHORE, S. N. : 1978, Thesis, University of Toronto.
SHORE, S. N., ADELMAN, S. J. : 1981, in *Upper Main Sequence Chemically Peculiar Stars,* 23rd Liege Astrophys. Coll., p. 429.
SHORE, S. N., BOLTON, C. T. : 1985, in preparation.
WALBORN, N. R. : 1983, *Astrophys. J.* **268,** 195.
WALBORN, N. R., HESSER, J. E. : 1976, *Astrophys. J. Lett.* **205,** L87.
WARREN, W. H., Jr., HESSER, J. E. : 1978, *Astrophys. J. Suppl.* **36,** 497.

TABLE I. — *Journal of spectrophotometric observations.*

Star	Scan	Heliocentric Julian Date (2440000.+)	Phase	Observer	Bandwidth (Å)
HR 1890	1	4568.841	0.256	SJA	30
	2	4569.801	0.322	SJA	30
	3	4570.772	0.399	SJA	30
	4	4570.840	0.474	SJA	30
	5	4570.902	0.543	SJA	30
	6	4570.961	0.608	SJA	30
	7	4571.930	0.684	SJA	30
	8	4572.815	0.665	SJA	30
	9	4572.894	0.754	SJA	30
	10	4574.872	0.949	SJA	30
	11	4574.934	0.018	SJA	30
	12	4655.607	0.534	SJA/DMP	20
σ Ori E	1	3442.963	0.725	SJA	30
	2	3585.617	0.521	SJA	30
	3	4568.790	0.155	SJA	30
	4	4568.874	0.225	SJA	30
	5	4568.949	0.288	SJA	30
	6	4570.851	0.885	SJA	30
	7	4570.916	0.940	SJA	30
	8	4571.880	0.749	SJA	30
	9	4572.786	0.510	SJA	30
σ Ori E	10	4572.854	0.567	SJA	30
	11	4574.845	0.239	SJA	30
	12	4574.908	0.292	SJA	30
	13	4655.625	0.075	SJA/DMP	20
	14	4655.906	0.143	SJA/DMP	20
HD 37776	1	4568.823	0.034	SJA	30
	2	4568.910	0.090	SJA	30
	3	4569.819	0.681	SJA	30
	4	4570.814	0.327	SJA	30
	5	4570.882	0.372	SJA	30
	6	4570.947	0.412	SJA	30
	7	4571.916	0.044	SJA	30
	8	4571.957	0.070	SJA	30
	9	4572.771	0.600	SJA	30
	10	4572.840	0.645	SJA	30
	11	4572.918	0.695	SJA	30
	12	4574.830	0.938	SJA	30
	13	4574.892	0.975	SJA	30
	14	4654.612	0.791	SJA/DMP	20
	15	4654.693	0.843	SJA/DMP	20
	16	4655.654	0.468	SJA/DMP	20
	17	4655.732	0.519	SJA/DMP	20

TABLE II. — *Continuous energy distributions* ($-$ 2.5 log F_{ν}/F_{5000}) *for HR 1890.*

λ(Å)	Scan 1	Scan 2	Scan 3	Scan 4	Scan 5	Scan 6	Scan 7
3300	-0.046	-0.015	-0.026	-0.027	-0.018	-0.027	-0.065
3360	-0.002	-0.004	-0.017	-0.021	-0.017	-0.020	-0.048
3390	-0.030	0.004	-0.017	-0.009	-0.024	-0.030	-0.044
3420	-0.019	0.017	0.002	0.004	-0.005	-0.006	-0.031
3448	0.012	0.034	0.032	0.025	0.001	0.013	-0.006
3478	0.004	0.030	0.006	0.018	0.005	0.010	-0.010
3509	0.007	0.030	0.018	0.012	0.007	-0.010	-0.009
3540	0.044	0.036	0.038	0.023	0.024	0.009	-0.011
3571	0.001	0.015	0.030	0.015	0.004	0.007	-0.001
3636	0.027	0.039	0.042	0.028	0.034	0.023	0.013
3704	0.048	0.054	0.057	0.056	0.032	0.052	0.013
4032	-0.231	-0.212	-0.205	-0.222	-0.227	-0.224	-0.240
4055	-0.304	-0.293	-0.299	-0.299	-0.304	-0.291	-0.309
4167	-0.256	-0.229	-0.246	-0.241	-0.247	-0.239	-0.255
4200	-0.242	-0.243	-0.232	-0.243	-0.254	-0.251	-0.253
4255	-0.232	-0.222	-0.229	-0.228	-0.226	-0.228	-0.245
4340	0.028	0.042	0.034	0.037	0.033	0.013	0.014
4412	-0.190	-0.172	-0.187	-0.172	-0.180	-0.181	-0.200
4464	-0.103	-0.107	-0.121	-0.127	-0.119	-0.120	-0.134
4566	-0.132	-0.140	-0.126	-0.133	-0.136	-0.134	-0.147
4673	-0.104	-0.107	-0.103	-0.104	-0.107	-0.109	-0.116
4785	-0.080	-0.076	-0.078	-0.074	-0.073	-0.080	-0.074
4861	0.148	0.170	0.156	0.168	0.159	0.169	0.143
4935	0.008	0.006	0.017	0.002	0.014	0.008	-0.009
4975	-0.012	-0.016	-0.019	-0.017	-0.024	-0.009	-0.035
5000	0.000	0.000	0.000	0.000	0.000	0.000	0.000
5060	0.028	0.018	0.037	0.013	0.028	0.026	0.021
5128	0.043	0.027	0.040	0.033	0.026	0.026	0.038
5200	0.052	0.037	0.062	0.047	0.036	0.062	0.050
5264	0.054	0.062	0.070	0.060	0.068	0.058	0.048
5360	0.080	0.092	0.088	0.078	0.082	0.077	0.073
5470	0.107	0.117	0.117	0.099	0.103	0.101	0.086
5556	0.129	0.137	0.134	0.127	0.127	0.140	0.121
5700	0.160	0.196	0.171	0.164	0.171	0.168	0.160
5800	0.201	0.245	0.228	0.210	0.219	0.230	0.207
5840	0.206	0.229	0.206	0.204	0.202	0.206	0.207
5875	0.251	0.269	0.252	0.252	0.253	0.266	0.267
6020	0.258	0.265	0.244	0.249	0.257	0.265	0.262
6058	0.257	0.288	0.284	0.251	0.259	0.275	0.262
6220	0.314	0.317	0.308	0.302	0.307	0.313	0.300
6370	0.338	0.347	0.334	0.329	0.324	0.349	0.334
6440	0.347	0.375	0.354	0.357	0.363	0.362	0.362
6563	0.478	0.501	0.469	0.473	0.473	0.479	0.474
6650	0.407	0.432	0.398	0.391	0.398	0.404	0.407
6710	0.402	0.426	0.406	0.403	0.419	0.415	0.402
6792	0.426	0.422	0.418	0.426	0.411	0.423	0.410
7102	0.479	0.478	0.473	0.472	0.472	0.496	0.485
u-b	0.225	0.248	0.236	0.235	0.231	0.230	0.215
b-y	-0.048	-0.060	-0.055	-0.045	-0.050	-0.052	-0.047
Δa	-0.002	-0.007	0.003	0.001	-0.004	0.001	0.003
ah′	0.043	0.024	0.065	0.032	0.058	0.012	0.093
ih*	0.023	0.037	0.033	0.031	0.023	0.013	0.029
hb	0.184	0.205	0.186	0.204	0.188	0.205	0.184
h_1	0.058	0.049	0.036	0.026	0.039	0.038	0.040
h_2	0.054	0.052	0.066	0.048	0.063	0.053	0.046
h_3	0.006	0.009	0.012	0.011	0.018	0.003	0.028

λ(Å)	Scan 8	Scan 9	Scan 10	Scan 11	Scan 12	Average	Dereddened Average
3300	-0.035	-0.049	-0.051	-0.008	-0.020	-0.032	-0.132
3360	-0.020	-0.034	-0.036	-0.047	-0.006	-0.023	-0.119
3390	-0.025	-0.031	-0.046	-0.046	0.000	-0.025	-0.119
3420	-0.004	-0.023	-0.025	-0.031	0.003	-0.010	-0.101
3448	0.013	0.001	-0.006	-0.006	0.032	0.012	-0.077
3478	0.005	-0.021	-0.016	-0.020	0.014	0.002	-0.084
3509	0.006	0.005	-0.011	-0.023	0.025	0.005	-0.079
3540	0.022	0.004	0.002	0.001	0.022	0.018	-0.065
3571	0.014	-0.008	-0.027	-0.022	0.024	0.004	-0.078
3636	0.029	0.012	0.019	0.008	0.061	0.028	-0.049
3704	0.044	0.018	0.018	0.007	0.080	0.040	-0.032
4032	-0.221	-0.226	-0.219	-0.213	-0.175	-0.218	-0.270
4055	-0.293	-0.298	-0.302	-0.311	-0.297	-0.300	-0.350
4167	-0.241	-0.251	-0.235	-0.247	-0.228	-0.243	-0.284
4200	-0.245	-0.253	-0.252	-0.263	-0.254	-0.249	-0.289
4255	-0.221	-0.241	-0.231	-0.243	-0.218	-0.230	-0.268
4340	0.036	0.015	-0.003	0.005	0.125	0.032	0.001
4412	-0.197	-0.192	-0.203	-0.198	-0.183	-0.188	-0.216
4464	-0.118	-0.120	-0.099	-0.091	-0.145	-0.117	-0.142
4566	-0.140	-0.148	-0.156	-0.155	-0.138	-0.140	-0.160
4673	-0.100	-0.116	-0.120	-0.121	-0.103	-0.109	-0.126
4785	-0.075	-0.093	-0.076	-0.087	-0.077	-0.079	-0.091
4861	0.168	0.148	0.126	0.138	0.236	0.161	0.153
4935	0.012	0.010	-0.005	-0.001	0.017	0.007	0.004
4975	-0.013	-0.033	-0.039	-0.041	-0.016	-0.022	-0.024
5000	0.000	0.000	0.000	0.000	0.000	0.000	0.000
5060	0.036	0.017	0.013	0.018	0.027	0.024	0.028
5128	0.040	0.023	0.014	0.010	0.035	0.030	0.038
5200	0.037	0.038	0.044	0.043	0.052	0.047	0.060
5264	0.059	0.050	0.062	0.066	0.066	0.060	0.077
5360	0.080	0.076	0.077	0.075	0.092	0.081	0.104
5470	0.124	0.099	0.112	0.105	0.118	0.107	0.137
5556	0.136	0.127	0.122	0.126	0.139	0.130	0.165
5700	0.178	0.170	0.166	0.170	0.179	0.171	0.212
5800	0.224	0.207	0.213	0.210	0.217	0.218	0.264
5840	0.204	0.196	0.213	0.214	0.212	0.208	0.256
5875	0.248	0.252	0.253	0.251	0.258	0.256	0.305
6020	0.258	0.247	0.239	0.252	0.243	0.253	0.306
6058	0.261	0.266	0.250	0.258	0.272	0.265	0.319
6220	0.308	0.300	0.294	0.298	0.302	0.305	0.360
6370	0.343	0.328	0.335	0.342	0.327	0.336	0.397
6440	0.362	0.338	0.351	0.338	0.348	0.355	0.422
6563	0.468	0.463	0.455	0.473	0.510	0.476	0.542
6650	0.397	0.393	0.410	0.400	0.404	0.403	0.475
6710	0.399	0.391	0.395	0.401	0.399	0.405	0.476
6792	0.416	0.420	0.398	0.408	0.419	0.476	0.489
7102	0.475	0.465	0.473	0.473	0.470	0.476	0.558
u-b	0.228	0.225	0.220	0.229	0.246	0.231	0.159
b-y	-0.055	-0.056	-0.061	-0.062	-0.061	-0.054	-0.099
Δa	-0.011	-0.005	0.001	0.002	-0.002	-0.002	0.002
ah′	0.048	0.067	0.071	0.075	0.040	0.041	0.052
ih*	0.023	0.017	0.044	0.033	0.032	0.028	0.031
hb	0.199	0.189	0.166	0.182	...	...	...
h_1	0.051	0.050	0.081	0.086	0.016	(0.047)	(0.046)
h_2	0.056	0.073	0.053	0.063	0.064	0.058	0.062
h_3	0.007	0.026	0.032	0.034	0.009	0.015	0.016

Note: Scan 12 has two additional values λ7530, m=0.570 & λ7859, m=0.611.

TABLE III. — *Continuous energy distributions* ($-2.5 \log F_\nu/F_{5000}$) *for σ Ori E.*

λ(Å)	Scan 1[1]	Scan 2[2]	Scan 3	Scan 4	Scan 5	Scan 6	Scan 7	Scan 8
3300	-0.206	-0.235	-0.197	-0.196	-0.200	-0.199	-0.194	-0.236
3360	...	...	-0.195	-0.199	-0.184	-0.180	-0.174	-0.223
3390	-0.188	-0.209	-0.179	-0.199	-0.178	-0.167	-0.172	-0.208
3420	...	...	-0.174	-0.178	-0.164	-0.174	-0.162	-0.204
3448	-0.154	-0.183	-0.153	-0.168	-0.143	-0.139	-0.112	-0.180
3471	...	...	-0.152	-0.152	-0.156	-0.163	-0.143	-0.193
3509	-0.158	-0.176	-0.141	-0.159	-0.142	-0.148	-0.158	-0.180
3540	...	...	-0.147	-0.141	-0.126	-0.166	-0.136	-0.161
3571	-0.186	-0.167	-0.161	-0.161	-0.136	-0.186	-0.171	-0.179
3636	-0.163	-0.138	-0.148	-0.135	-0.119	-0.160	-0.121	-0.157
3704	-0.132	-0.122	-0.108	-0.124	-0.088	-0.114	-0.116	-0.136
4032	-0.227	-0.270	-0.242	-0.237	-0.242	-0.194	-0.206	-0.228
4055	-0.313	-0.338	-0.307	-0.318	-0.316	-0.308	-0.313	-0.332
4167	-0.254	-0.268	-0.269	-0.266	-0.223	-0.252	-0.259	-0.270
4200	-0.250	-0.272	-0.271	-0.257	-0.256	-0.261	-0.273	-0.260
4255	-0.229	-0.264	-0.249	-0.250	-0.223	-0.243	-0.239	-0.256
4340	...	...	-0.052	-0.046	-0.036	-0.075	-0.060	-0.082
4412	-0.187	-0.210	-0.192	-0.209	-0.185	-0.193	-0.199	-0.229
4464	-0.095	-0.139	-0.129	-0.133	-0.119	-0.081	-0.099	-0.121
4566	-0.145	-0.160	-0.143	-0.147	-0.129	-0.157	-0.148	-0.170
4673	-0.107	-0.128	-0.114	-0.128	-0.096	-0.112	-0.117	-0.129
4785	-0.076	-0.082	-0.081	-0.089	-0.065	-0.069	-0.093	-0.096
4861	...	...	0.087	0.089	0.102	0.073	0.083	0.045
4935	0.015	-0.013	-0.002	-0.003	0.025	0.008	0.001	0.003
4975	0.004	-0.033	-0.035	-0.036	-0.016	-0.030	-0.024	-0.036
5000	0.000	0.000	0.000	0.000	0.000	0.000	0.000	0.000
5060	...	...	0.027	0.008	0.049	0.028	0.025	0.021
5128	0.038	0.023	0.035	0.029	0.038	0.021	0.031	0.027
5200	0.050	0.037	0.041	0.032	0.046	0.046	0.044	0.036
5264	0.062	0.058	0.046	0.056	0.084	0.062	0.062	0.046
5360	0.094	0.084	0.088	0.084	0.092	0.082	0.084	0.069
5470	0.111	0.111	0.125	0.115	0.135	0.128	0.108	0.097
5556	0.142	0.130	0.136	0.121	0.145	0.139	0.132	0.113
5700	0.170	0.168	0.177	0.160	0.194	0.173	0.170	0.159
5800	0.218	0.209	0.212	0.204	0.234	0.227	0.215	0.201
5840	0.223	0.206	0.226	0.196	0.221	0.218	0.220	0.197
5875	...	...	0.268	0.247	0.279	0.281	0.260	0.254
6020	0.262	0.254	0.258	0.246	0.268	0.263	0.244	0.244
6058	...	...	0.279	0.248	0.278	0.272	0.267	0.246
6220	0.307	0.295	0.309	0.306	0.335	0.306	0.306	0.294
6370	0.338	0.351	0.347	0.331	0.365	0.338	0.334	0.322
6440	...	...	0.373	0.345	0.386	0.364	0.348	0.344
6563	...	...	0.428	0.408	0.442	0.391	0.416	0.364
6650	0.413	0.416	0.412	0.409	0.432	0.412	0.407	0.390
6710	...	0.419	0.419	0.403	0.429	0.405	0.402	0.395
6792	0.434	0.428	0.427	0.415	0.447	0.432	0.419	0.417
7102	0.489	0.486	0.482	0.469	0.502	0.479	0.487	0.458
u-b	0.056	0.060	0.073	0.078	0.065	0.066	0.083	0.060
b-y	-0.060	-0.072	-0.065	-0.067	-0.061	-0.066	-0.064	-0.063
Δa	-0.004	-0.002	-0.010	-0.004	-0.005	-0.006	-0.001	-0.004
ah′	...	...	0.090	0.074	0.062	0.063	0.057	0.080
ih*	0.038	0.046	-0.009	0.027	0.059	0.027	0.011	0.053
hb	...	...	0.129	0.135	0.122	0.104	0.129	0.092
h_1	0.071	0.046	0.039	0.045	0.038	0.094	0.075	0.079
h_2	0.051	0.045	0.056	0.060	0.066	0.058	0.060	0.069
h_3	-0.010	0.026	0.028	0.029	0.009	0.023	0.017	0.029

λ(Å)	Scan 9	Scan 10	Scan 11	Scan 12	Scan 13[3]	Scan 14[4]	Average	Dereddened Average
3300	-0.181	-0.201	-0.222	-0.182	-0.128	-0.193	-0.198	-0.298
3360	-0.160	-0.190	-0.183	-0.162	-0.108	-0.176	-0.182	-0.278
3390	-0.159	-0.181	-0.191	-0.157	-0.106	-0.182	-0.177	-0.271
3420	-0.150	-0.170	-0.178	-0.154	-0.094	-0.170	-0.168	-0.260
3448	-0.123	-0.162	-0.164	-0.125	-0.073	-0.147	-0.146	-0.234
3471	-0.129	-0.164	-0.159	-0.127	-0.078	-0.160	-0.152	-0.239
3509	-0.126	-0.147	-0.162	-0.100	-0.064	-0.138	-0.143	-0.227
3540	-0.122	-0.156	-0.145	-0.095	-0.085	-0.152	-0.140	-0.222
3571	-0.118	-0.150	-0.146	-0.113	-0.103	-0.173	-0.154	-0.235
3636	-0.087	-0.140	-0.138	-0.098	-0.027	-0.143	-0.127	-0.205
3704	-0.082	-0.111	-0.105	-0.084	-0.053	-0.113	-0.106	-0.183
4032	-0.249	-0.240	-0.249	-0.206	-0.172	-0.212	-0.227	-0.276
4055	-0.304	-0.313	-0.322	-0.297	-0.307	-0.326	-0.315	-0.365
4167	-0.240	-0.246	-0.271	-0.237	-0.244	-0.262	-0.254	-0.296
4200	-0.244	-0.234	-0.279	-0.234	-0.248	-0.276	-0.258	-0.298
4255	-0.234	-0.235	-0.251	-0.217	-0.245	-0.239	-0.241	-0.279
4340	-0.037	-0.031	-0.050	-0.014	0.031	0.007	...	...
4412	-0.194	-0.173	-0.191	-0.187	-0.184	-0.208	-0.196	-0.224
4464	-0.126	-0.121	-0.116	-0.116	-0.136	-0.130	-0.119	-0.144
4566	-0.153	-0.135	-0.159	-0.148	-0.140	-0.160	-0.150	-0.171
4673	-0.100	-0.107	-0.115	-0.104	-0.119	-0.124	-0.114	-0.130
4785	-0.079	-0.075	-0.088	-0.070	-0.079	-0.084	-0.080	-0.092
4861	0.100	0.106	0.076	0.101	0.179	0.145	...	...
4935	0.018	0.017	-0.016	0.011	0.020	-0.003	0.006	0.002
4975	-0.024	-0.020	-0.028	-0.010	-0.004	-0.024	-0.023	-0.025
5000	0.000	0.000	0.000	0.000	0.000	0.000	0.000	0.000
5060	0.035	0.030	0.021	0.024	0.028	0.017	0.026	0.030
5128	0.040	0.048	0.029	0.030	0.038	0.026	0.032	0.042
5200	0.041	0.036	0.051	0.051	0.051	0.028	0.042	0.056
5264	0.074	0.070	0.060	0.064	0.064	0.060	0.062	0.080
5360	0.094	0.092	0.084	0.084	0.088	0.089	0.086	0.108
5470	0.113	0.131	0.104	0.116	0.131	0.115	0.117	0.147
5556	0.149	0.150	0.127	0.125	0.131	0.128	0.133	0.167
5700	0.191	0.183	0.172	0.175	0.182	0.180	0.175	0.217
5800	0.231	0.223	0.225	0.224	0.216	0.206	0.218	0.264
5840	0.221	0.215	0.209	0.214	0.205	0.204	0.212	0.260
5875	0.289	0.273	0.248	0.266	0.292	0.272	0.269	0.319
6020	0.270	0.260	0.247	0.267	0.279	0.261	0.259	0.312
6058	0.290	0.281	0.248	0.283	0.277	0.264	0.270	0.324
6220	0.318	0.318	0.294	0.322	0.320	0.311	0.288	0.345
6370	0.353	0.355	0.320	0.355	0.356	0.341	0.343	0.404
6440	0.378	0.361	0.345	0.364	0.373	0.351	0.361	0.424
6563	0.435	0.426	0.405	0.440	0.466	0.409	...	...
6650	0.427	0.398	0.400	0.441	0.417	0.389	0.412	0.481
6710	0.442	0.416	0.400	0.438	0.415	0.403	0.414	0.484
6792	0.444	0.434	0.418	0.462	0.433	0.436	0.432	0.506
7102	0.511	0.501	0.467	0.525	0.502	0.482	0.489	0.570
u-b	0.095	0.063	0.071	0.097	0.149	0.083	0.078	0.006
b-y	-0.065	-0.067	-0.063	-0.055	-0.070	-0.072	-0.065	-0.109
Δa	-0.004	-0.009	0.004	-0.002	-0.005	-0.007	-0.004	0.000
ah′	0.069	0.061	0.064	0.023	0.017	0.046	0.056	0.060
ih*	0.048	0.056	0.012	0.048	0.038	0.031	0.035	0.038
hb	0.131	0.135	0.128	0.131	0.209	0.189	...	...
h_1	0.048	0.033	0.059	0.052	0.026	0.054	(0.054)	(0.054)
h_2	0.070	0.065	0.042	0.051	0.062	0.051	0.058	0.061
h_3	0.017	0.013	0.021	0.004	-0.002	0.017	0.016	0.017

Notes: [1] Additional values: λ6300, m = 0.330; λ6620, m = 0.389
[2] Additional value: λ6300, m = 0.325
[3] Additional values: λ7530, m = 0.593; λ7850, m = 0.665
[4] Additional values: λ7530, m = 0.553; λ7850, m = 0.600

TABLE IV. — *Continuous energy distributions* ($-2.5 \log F_{\nu}/F_{5000}$) *for HD 37776.*

λ(Å)	Scan 1	Scan 2	Scan 3	Scan 4	Scan 5	Scan 6	Scan 7	Scan 8	Scan 9	Scan 10
3300	-0.139	-0.126	-0.144	-0.131	-0.131	-0.145	-0.167	-0.156	-0.147	-0.143
3360	-0.137	-0.121	-0.148	-0.117	-0.129	-0.140	-0.155	-0.133	-0.117	-0.122
3390	-0.142	-0.107	-0.135	-0.113	-0.126	-0.142	-0.146	-0.131	-0.115	-0.126
3420	-0.127	-0.108	-0.120	-0.104	-0.121	-0.127	-0.136	-0.116	-0.105	-0.117
3448	-0.105	-0.085	-0.104	-0.081	-0.089	-0.106	-0.115	-0.097	-0.084	-0.100
3478	-0.109	-0.094	-0.113	-0.093	-0.100	-0.108	-0.117	-0.100	-0.099	-0.106
3509	-0.087	-0.082	-0.101	-0.081	-0.104	-0.114	-0.118	-0.101	-0.082	-0.091
3540	-0.086	-0.082	-0.099	-0.078	-0.084	-0.098	-0.091	-0.088	-0.079	-0.086
3571	-0.092	-0.074	-0.113	-0.100	-0.104	-0.108	-0.102	-0.079	-0.103	-0.112
3636	-0.067	-0.063	-0.086	-0.064	-0.079	-0.105	-0.082	-0.075	-0.070	-0.090
3704	-0.048	-0.040	-0.063	-0.046	-0.061	-0.072	-0.054	-0.058	-0.064	-0.064
4032	-0.248	-0.228	-0.215	-0.192	-0.224	-0.241	-0.271	-0.250	-0.198	-0.214
4055	-0.316	-0.304	-0.304	-0.292	-0.292	-0.304	-0.307	-0.300	-0.295	-0.300
4167	-0.251	-0.248	-0.247	-0.233	-0.245	-0.251	-0.248	-0.240	-0.250	-0.242
4200	-0.260	-0.237	-0.255	-0.249	-0.259	-0.260	-0.250	-0.248	-0.248	-0.241
4255	-0.223	-0.214	-0.221	-0.220	-0.233	-0.227	-0.241	-0.229	-0.222	-0.231
4340	-0.005	-0.004	-0.029	-0.035	-0.047	-0.040	-0.021	-0.009	-0.039	-0.042
4412	-0.195	-0.178	-0.175	-0.175	-0.184	-0.205	-0.199	-0.195	-0.177	-0.189
4464	-0.139	-0.117	-0.099	-0.098	-0.103	-0.126	-0.152	-0.142	-0.096	-0.119
4566	-0.133	-0.136	-0.143	-0.137	-0.141	-0.147	-0.154	-0.137	-0.141	-0.148
4673	-0.113	-0.113	-0.115	-0.099	-0.109	-0.117	-0.129	-0.113	-0.108	-0.103
4785	-0.082	-0.086	-0.084	-0.074	-0.081	-0.095	-0.095	-0.081	-0.078	-0.097
4861	0.115	0.115	0.091	0.086	0.100	0.076	0.111	0.116	0.085	0.071
4935	-0.019	-0.013	0.006	0.024	0.009	0.004	-0.026	-0.009	0.016	0.021
4975	-0.028	-0.031	-0.026	-0.029	-0.032	-0.041	-0.043	-0.024	-0.031	-0.026
5000	0.000	0.000	0.000	0.000	0.000	0.000	0.000	0.000	0.000	0.000
5060	0.008	0.023	0.021	0.023	0.022	0.010	0.014	0.027	0.017	0.018
5128	0.027	0.038	0.019	0.037	0.023	0.006	0.026	0.040	0.020	0.018
5200	0.038	0.042	0.042	0.042	0.036	0.040	0.029	0.043	0.029	0.034
5264	0.052	0.061	0.044	0.052	0.046	0.040	0.049	0.062	0.044	0.050
5360	0.070	0.078	0.072	0.075	0.079	0.066	0.074	0.080	0.067	0.068
5470	0.113	0.104	0.097	0.112	0.087	0.105	0.092	0.100	0.094	0.104
5556	0.121	0.113	0.108	0.129	0.123	0.116	0.106	0.125	0.122	0.111
5700	0.160	0.167	0.156	0.168	0.154	0.148	0.155	0.168	0.154	0.146
5800	0.202	0.202	0.197	0.205	0.206	0.196	0.204	0.222	0.200	0.189
5840	0.196	0.186	0.194	0.207	0.194	0.189	0.196	0.204	0.195	0.186
5875	0.244	0.253	0.248	0.248	0.259	0.241	0.234	0.264	0.248	0.249
6020	0.238	0.243	0.238	0.259	0.235	0.236	0.238	0.245	0.244	0.239
6058	0.247	0.257	0.237	0.254	0.250	0.238	0.245	0.263	0.253	0.248
6220	0.291	0.294	0.277	0.292	0.272	0.282	0.285	0.293	0.289	0.285
6370	0.336	0.331	0.300	0.334	0.319	0.315	0.328	0.338	0.312	0.307
6440	0.349	0.341	0.315	0.332	0.339	0.331	0.342	0.353	0.332	0.333
6563	0.421	0.421	0.402	0.403	0.403	0.394	0.430	0.439	0.407	0.395
6650	0.398	0.397	0.387	0.391	0.380	0.397	0.387	0.410	0.384	0.374
6710	0.385	0.386	0.363	0.391	0.381	0.376	0.366	0.387	0.385	0.387
6792	0.416	0.407	0.386	0.418	0.398	0.400	0.403	0.417	0.388	0.388
7102	0.464	0.452	0.438	0.457	0.465	0.451	0.470	0.481	0.462	0.454
u-b	0.127	0.142	0.121	0.128	0.127	0.123	0.128	0.126	0.127	0.125
b-y	-0.052	-0.051	-0.044	-0.045	-0.042	-0.052	-0.058	-0.053	-0.039	-0.045
Δa	-0.003	0.002	-0.005	-0.007	-0.006	-0.006	0.000	0.001	-0.010	-0.007
ah′	0.052	0.089	0.057	0.075	0.071	0.068	0.102	0.072	0.061	0.052
ih*	0.029	0.039	0.025	0.024	0.004	0.018	0.039	0.030	0.014	0.041
hb	0.165	0.164	0.130	0.111	0.136	0.121	0.171	0.161	0.116	0.133
h_1	0.025	0.045	0.060	0.058	0.060	0.050	0.025	0.024	0.063	0.050
h_2	0.036	0.046	0.061	0.076	0.066	0.072	0.043	0.044	0.071	0.083
h_3	0.022	0.025	0.020	0.022	0.025	0.034	0.037	0.018	0.024	0.020

λ(Å)	Scan 11	Scan 12	Scan 13	Scan 14	Scan 15	Scan 16	Scan 17	Average	Dereddened Average
3300	-0.128	-0.144	-0.152	-0.134	-0.125	-0.130	-0.142	-0.141	-0.275
3360	-0.117	-0.129	-0.133	-0.129	-0.136	-0.109	-0.106	-0.129	-0.258
3390	-0.111	-0.126	-0.123	-0.123	-0.130	-0.112	-0.109	-0.125	-0.251
3420	-0.103	-0.112	-0.123	-0.111	-0.116	-0.110	-0.118	-0.117	-0.239
3448	-0.089	-0.093	-0.099	-0.084	-0.087	-0.079	-0.082	-0.093	-0.211
3478	-0.082	-0.098	-0.099	-0.098	-0.106	-0.086	-0.094	-0.101	-0.216
3509	-0.083	-0.082	-0.093	-0.087	-0.096	-0.066	-0.088	-0.092	-0.204
3540	-0.068	-0.077	-0.089	-0.074	-0.089	-0.087	-0.098	-0.086	-0.197
3571	-0.091	-0.078	-0.071	-0.081	-0.094	-0.114	-0.106	-0.096	-0.205
3636	-0.070	-0.062	-0.066	-0.052	-0.039	-0.029	-0.042	-0.068	-0.171
3704	-0.049	-0.048	-0.049	-0.025	-0.021	-0.035	-0.048	-0.050	-0.147
4032	-0.202	-0.247	-0.251	-0.196	-0.211	-0.179	-0.161	-0.219	-0.288
4055	-0.284	-0.292	-0.306	-0.308	-0.300	-0.293	-0.302	-0.300	-0.366
4167	-0.228	-0.238	-0.232	-0.240	-0.233	-0.244	-0.233	-0.241	-0.296
4200	-0.222	-0.238	-0.245	-0.234	-0.234	-0.232	-0.244	-0.245	-0.297
4255	-0.212	-0.214	-0.221	-0.225	-0.217	-0.213	-0.224	-0.223	-0.273
4340	-0.023	0.005	0.006	0.047	0.074	0.042	0.022	-0.006	-0.048
4412	-0.174	-0.178	-0.184	-0.164	-0.165	-0.181	-0.178	-0.182	-0.220
4464	-0.094	-0.138	-0.138	-0.168	-0.153	-0.127	-0.143	-0.127	-0.161
4566	-0.120	-0.121	-0.134	-0.126	-0.118	-0.136	-0.138	-0.136	-0.163
4673	-0.089	-0.108	-0.111	-0.103	-0.093	-0.094	-0.108	-0.107	-0.129
4785	-0.074	-0.077	-0.087	-0.072	-0.072	-0.067	-0.070	-0.081	-0.098
4861	0.100	0.139	0.127	0.140	0.181	0.169	0.152	0.116	0.105
4935	0.031	-0.003	-0.017	0.048	0.005	0.014	0.013	0.006	0.001
4975	0.000	-0.030	-0.025	-0.023	-0.015	-0.010	-0.008	-0.025	-0.027
5000	0.000	0.000	0.000	0.000	0.000	0.000	0.000	0.000	0.000
5060	0.035	0.013	0.009	0.029	0.012	0.019	0.026	0.019	0.025
5128	0.033	0.035	0.037	0.037	0.047	0.035	0.036	0.030	0.042
5200	0.048	0.045	0.044	0.036	0.049	0.036	0.045	0.040	0.058
5264	0.072	0.066	0.066	0.050	0.068	0.062	0.051	0.055	0.078
5360	0.086	0.090	0.083	0.082	0.084	0.086	0.095	0.079	0.110
5470	0.117	0.104	0.106	0.095	0.108	0.106	0.116	0.104	0.142
5556	0.134	0.135	0.131	0.129	0.131	0.127	0.132	0.124	0.170
5700	0.185	0.171	0.162	0.164	0.183	0.167	0.157	0.163	0.217
5800	0.215	0.212	0.206	0.208	0.215	0.205	0.190	0.205	0.266
5840	0.214	0.216	0.194	0.186	0.194	0.206	0.194	0.198	0.261
5875	0.259	0.262	0.255	0.255	0.257	0.267	0.273	0.254	0.319
6020	0.256	0.250	0.249	0.234	0.258	0.262	0.258	0.247	0.317
6058	0.259	0.254	0.265	0.253	0.264	0.253	0.262	0.254	0.326
6220	0.303	0.305	0.302	0.284	0.301	0.286	0.285	0.290	0.367
6370	0.337	0.349	0.338	0.327	0.338	0.315	0.325	0.327	0.409
6440	0.341	0.364	0.350	0.347	0.351	0.353	0.336	0.342	0.426
6563	0.424	0.454	0.436	0.447	0.452	0.459	0.453	0.426	0.515
6650	0.400	0.406	0.399	0.387	0.391	0.388	0.373	0.392	0.484
6710	0.404	0.400	0.401	0.376	0.388	0.394	0.391	0.387	0.491
6792	0.415	0.416	0.407	0.418	0.427	0.410	0.431	0.409	0.507
7102	0.466	0.473	0.473	0.465	0.477	0.462	0.465	0.464	0.572
7530	...	...	...	0.568	0.575	0.567	0.580	0.570	0.692
7850	...	...	...	0.596	0.633	0.633	0.606	0.614	0.747
u-b	0.120	0.127	0.129	0.130	0.121	0.129	0.130	0.126	0.030
b-y	-0.044	-0.052	-0.057	-0.042	-0.044	-0.044	-0.057	-0.049	-0.108
Δa	-0.005	0.002	0.004	-0.011	0.002	-0.006	-0.009	-0.004	0.002
ah′	0.007	0.063	0.050	0.066	0.038	0.022	0.023	0.057	0.059
ih*	0.036	0.022	0.048	0.050	0.041	0.031	0.045	0.032	0.037
hb	0.121	0.179	0.179	0.152	0.214	0.195	0.180	...	...
h_1	0.053	0.012	0.021	-0.023	-0.012	0.032	0.015	(0.032)	(0.031)
h_2	0.068	0.051	0.039	0.096	0.049	0.053	0.052	0.059	0.064
h_3	-0.006	0.023	0.018	0.016	0.009	0.004	0.002	0.019	0.019

TABLE V. — *Comparison of uvby photometry for helium and comparison stars.*

Star	HD Number	V	u-b	b-y	m_1	n	References
HR 1890	37017	6.556	0.244	-0.060	0.108	2	Gronbech and Olsen (1976)
		6.55	0.252	-0.057	0.104	1+	Warren and Hesser (1978)
		...	0.231	-0.054	...	12	This Paper: Spectrophotometry
		6.565	0.235	-0.062	0.101	21	This Paper: Photometry
	(σ)	(0.006)	(0.008)	(0.004)	(0.012)		
HR 1891	37016	6.255	0.321	-0.069	0.101	2	Gronbech and Olsen (1976)
		6.24	0.335	-0.060	0.100	1+	Warren and Hesser (1978)
		6.251	0.315	-0.068	0.098	20	This Paper: Photometry
	(σ)	(0.010)	(0.004)	(0.006)	(0.015)		
σ Ori E	37479	6.66	0.099	-0.072	0.097	3	Crawford et al. (1971)
		6.692	0.100	-0.062	0.090	2	Gronbech and Olsen (1976)
		6.68	0.099	-0.069	0.099	1+	Warren and Hesser (1978)
		...	0.078	-0.065	...	14	This Paper: Spectrophotometry
V901 Ori	37776	...	0.178	-0.074	0.134	4	Shaw (1975)
		6.98	0.150	-0.053	0.100	1+	Warren and Hesser (1978)
		7.01	0.147	-0.056	0.099	3	Kilkenney (1978)
		...	0.126	-0.049	...	17	This Paper: Spectrophotometry
		6.998	0.134	-0.054	0.080	18	This Paper: Photometry
	(σ)	(0.010)	(0.005)	(0.005)	(0.011)		
HR 1950	37744	6.22	0.021	-0.075	0.053	3	Crawford et al. (1971)
		6.216	0.043	-0.087	0.086	3	Gronbech and Olsen (1976)
		6.22	0.037	-0.077	0.073	1+	Warren and Hesser (1978)
		6.212	0.028	-0.089	0.085	18	This Paper: Photometry
	(σ)	(0.013)	(0.007)	(0.008)	(0.013)		

TABLE VI. — *Four-color photometry of the helium stars.*

Star	Julian Date (2440000.+)	Phase	Δ(b-y)	Δ(u-b)	Δy	Δv	β
HR 1890	4216.891	0.708	0.003	-0.076	0.300	0.321	2.640
	4217.880	0.806	0.004	-0.089	0.302	0.322	2.649
	4221.870	0.233	0.010	-0.086	0.324	0.343	2.645
	4222.846	0.316	0.008	-0.079	0.321	0.350	2.662
	4588.810	0.415	0.005:	-0.063:	0.319:	0.338:	2.644
	4589.812	0.527	0.004	-0.077	0.322	0.329	2.653
	4590.803	0.627	0.002	-0.077	0.315	0.316	2.630
	4927.876	0.666	0.011	-0.086	0.305	0.319	2.645
	4928.877	0.777	0.003	-0.092	0.307	0.322	2.642
	4931.859	0.086	0.006	-0.087	0.309	0.328	2.633
	4932.835	0.169	0.010	-0.087	0.314	0.332	2.640
	4933.857	0.303	0.013	-0.084	0.318	0.342	2.657
	4934.842	0.396	0.010	-0.074	0.317	0.345	2.654
	5619.955	0.644	0.003	-0.078	0.314	0.321	2.654
	5620.953	0.752	-0.001	-0.082	0.313	0.321	2.649
	5627.955	0.521	0.005	-0.077	0.317	0.337	...
	5782.634	0.164	0.005	-0.085	0.318	0.337	2.645
	5783.614	0.252	0.008	-0.079	0.317	0.337	2.650
	5785.610	0.467	0.011	-0.059	0.312	0.342	...
	5787.617	0.693	0.009	-0.084	0.307	0.316	...
	5987.944	0.991	0.003	-0.108	0.314	0.325	2.639
HD 37776	4217.904	0.960	0.039	0.101	0.773	0.828	2.641
	4222.885	0.197	0.040	0.109	0.785	0.858	2.591
	4588.838	0.042	0.040	0.116	0.776	0.843	2.609
	4589.834	0.689	0.037	0.111	0.787	0.846	2.595
	4590.825	0.333	0.038	0.104	0.795	0.871	2.604
	4927.906	0.413	0.028	0.105	0.794	0.865	2.612
	4928.908	0.065	0.033	0.110	0.785	0.846	2.634
	4931.889	0.002	0.025	0.111	0.780	0.829	2.624
	4932.884	0.649	0.036	0.102	0.790	0.865	2.606
	4933.889	0.302	0.039	0.104	0.798	0.861	2.619
	4934.860	0.933	0.035	0.112	0.768	0.833	2.635
	5619.972	0.210	0.040	0.099	0.796	0.856	2.623
	5620.970	0.859	0.025	0.108	0.785	0.842	2.644
	5627.972	0.410	0.039	0.104	0.787	0.861	2.606
	5782.649	0.938	0.040	0.102	0.769	0.835	...
	5783.626	0.574	0.036	0.105	0.793	0.873	...
	5785.622	0.871	0.035	0.109	0.780	0.840	...
	5987.970	0.384	0.032	0.097	0.798	0.868	2.594

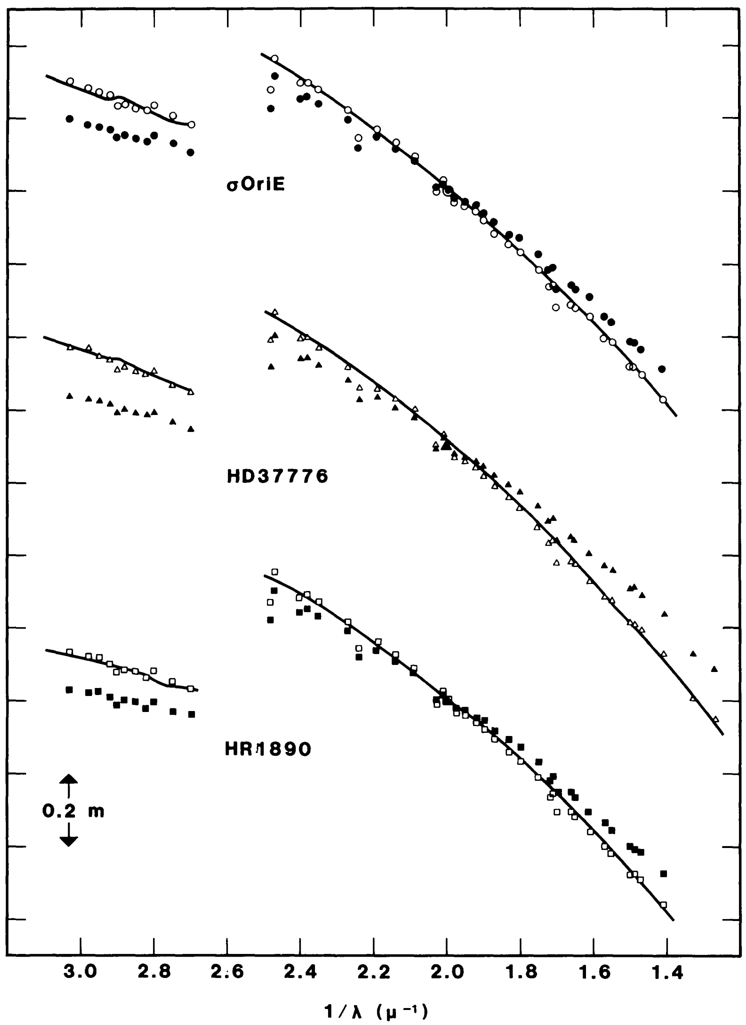

FIGURE 1. — The observed average energy distributions, normalized to $\lambda 5000$, of the three helium variables : σ Ori E (circles), HD 37776 (triangles), and HR 1890 (squares). In each case, solid symbols represent the raw data and open symbols the energy distributions corrected for reddening (see text). The solid lines represent the solar composition $\log g = 4.0$ model atmospheres predictions that best match the dereddened energy distributions. The effective temperatures of the models are : σ Ori E, 23400 K ; HD 37776, 22500 K, and HR 1890, 20000 K.

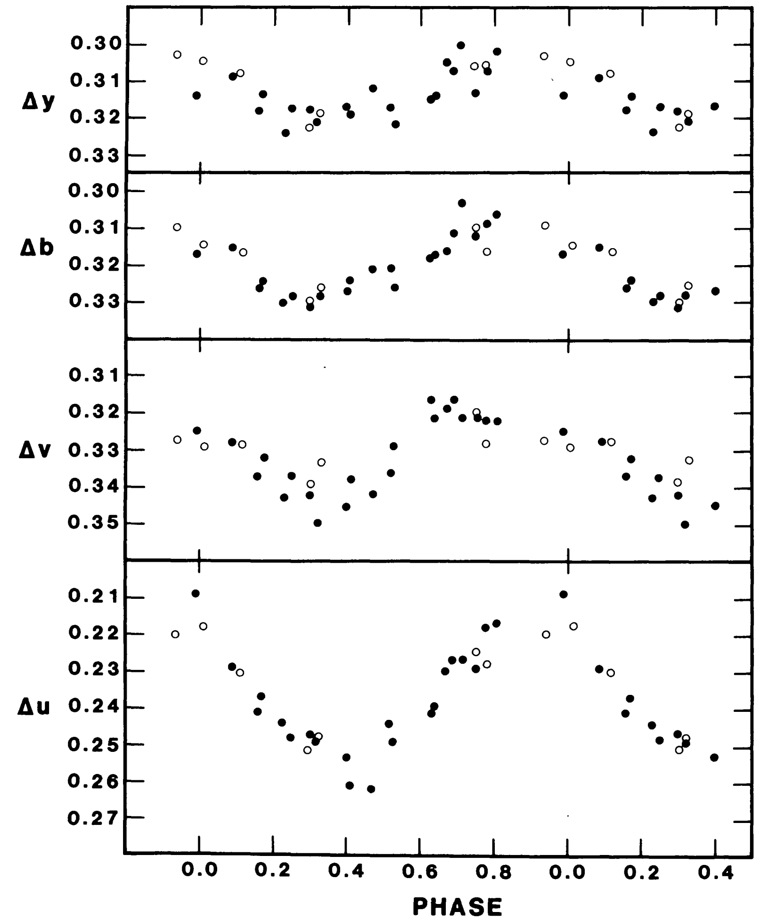

FIGURE 2. — Photometric variations with phase of HR 1890. Closed circles represent the 4-color photometry of DMP relative to the comparison star HR 1891. Open circles represent the 4-color photometry of Pedersen and Thomsen (1977) with an arbitrary shift in magnitude.

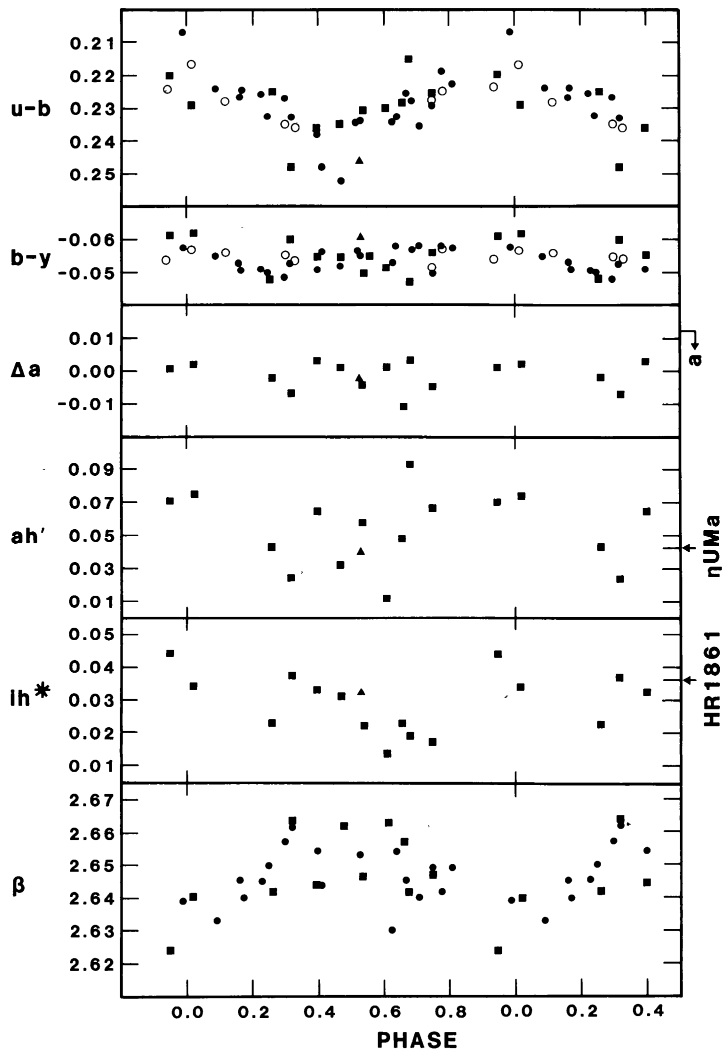

FIGURE 3. — The index values of HR 1890 as a function of phase. Closed squares are scans 1-11 and the closed triangle is scan 12. The other symbols are the same as in figure 2. In the bottom plot the scale is that of the 4-color photometry, while the closed squares represent the *hb* values with an arbitrary magnitude shift. The « a » in the right hand margin of the Δa plot indicates the value below which the $\lambda 5200$ feature is absent. The *ah′* value of η UMa and the *ih** value of HR 1861 are indicated in the right margin of the *ah′* and *ih** plots, respectively.

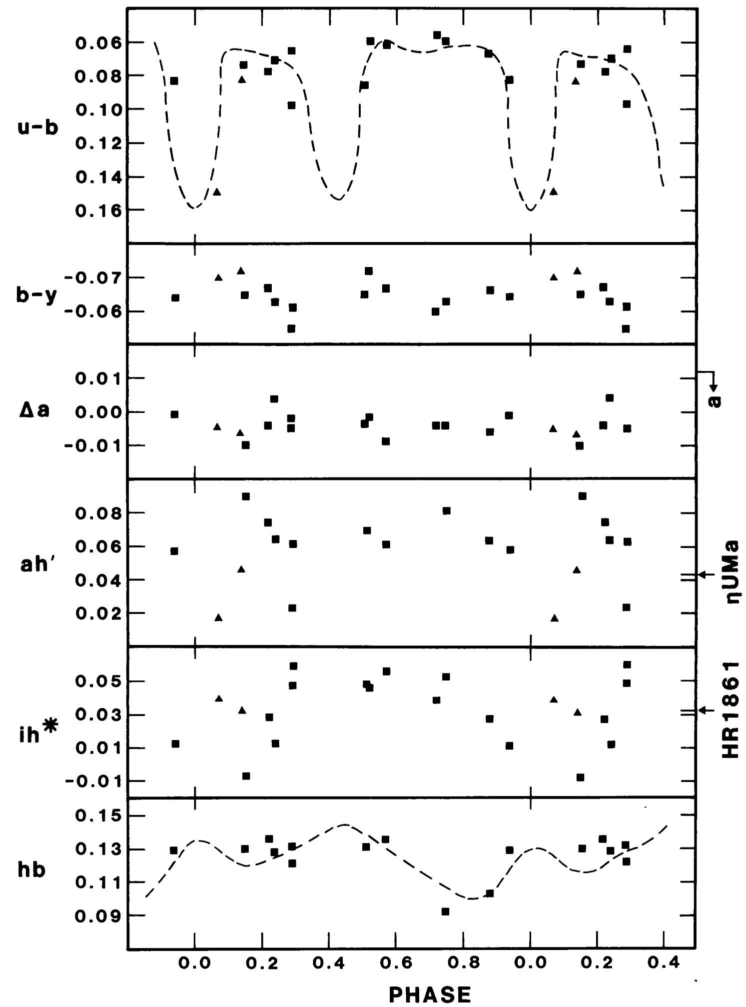

FIGURE 4. — The index values of σ Ori E as a function of phase. Closed squares represent scans 1-12 and closed triangles scans 13-14. In the top and bottom plots, respectively, the dashed lines represent the *u-b* and β values of Hesser *et al.* (1977) with arbitrary magnitude shifts. The right margin notations are as for figure 3.

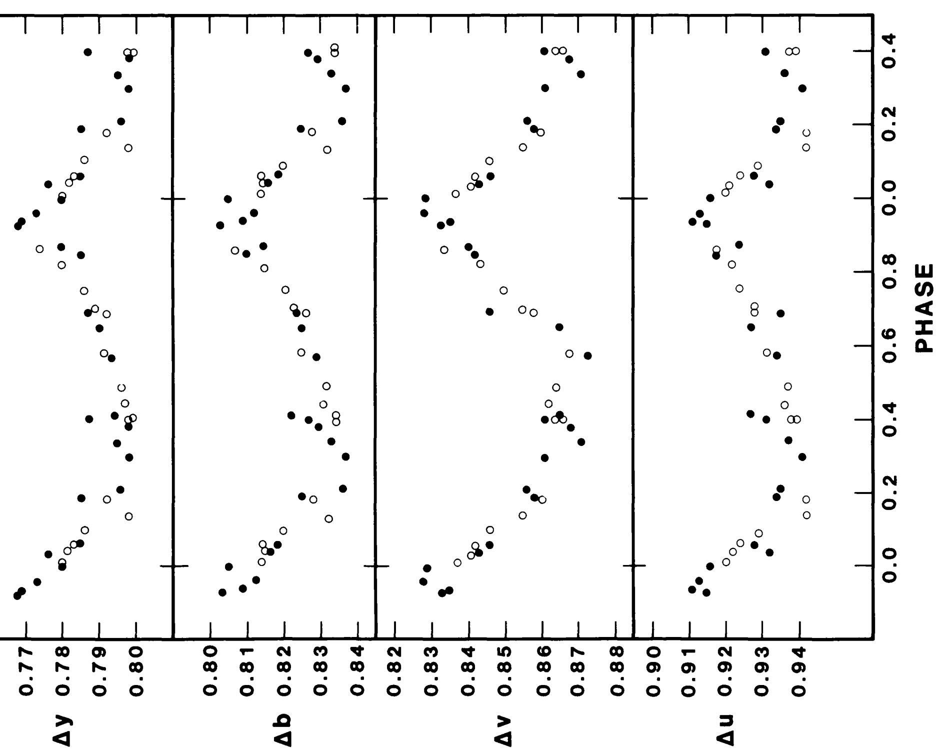

FIGURE 5. — Photometric variations with phase of HD 37776. The symbols are the same as in figure 2. Values of DMP are relative to the comparison star HR 1950.

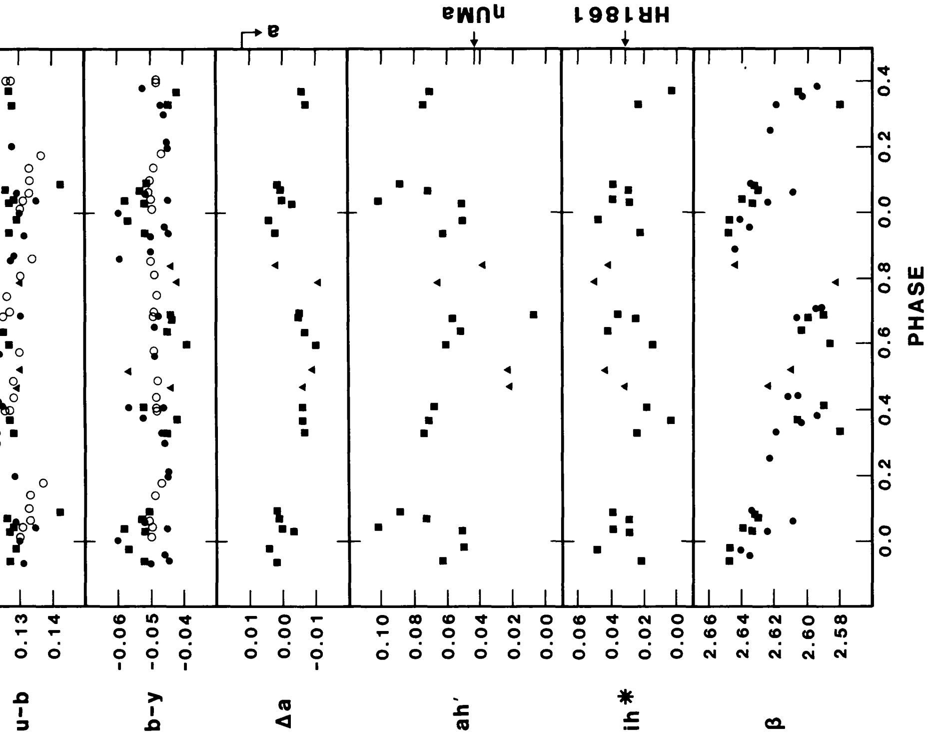

FIGURE 6. — The index values of HD 37776 as a function of phase. Closed squares are scans 1-13 and closed triangles, scans 14-17. The other symbols are the same as in figures 2 and 3.

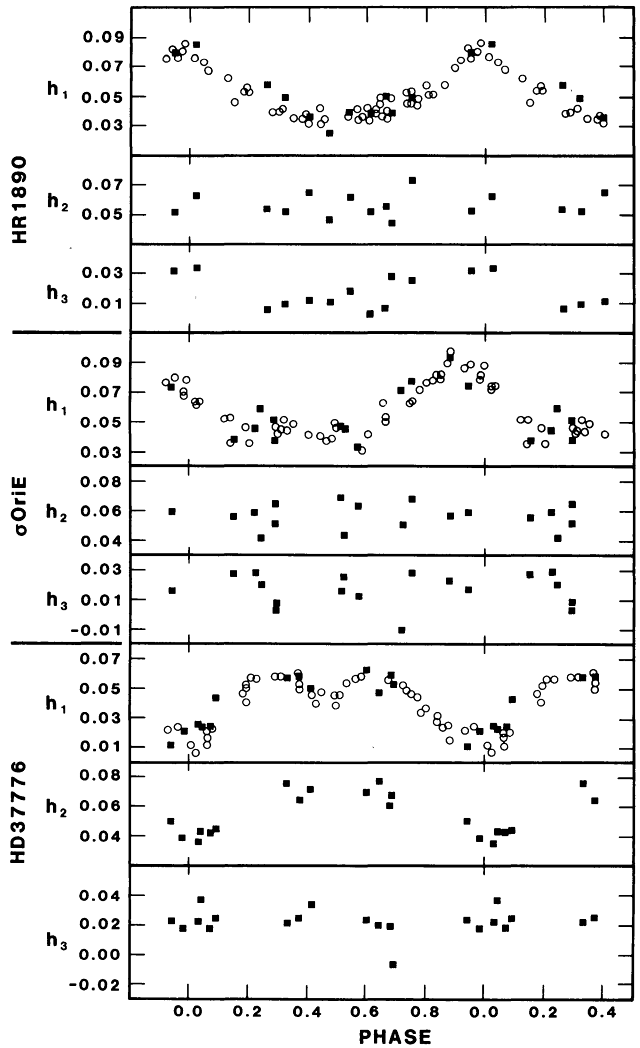

FIGURE 7. — The spectrophotometric indices h_1, h_2, and h_3 (closed squares) plotted as a function of phase for a) HR 1890, b) σ Ori E, and c) HD 37776. The open circles represent the R values for He I λ4026 of Pedersen and Thomsen (1977).